Analytical Biochemistry 388 (2009) 288–295

Contents lists available at ScienceDirect

Analytical Biochemistry

journal homepage: www.elsevier.com/locate/yabio

Multiwalled carbon nanotubes with poly(*NDGAChi*) biocomposite film for the electrocatalysis of epinephrine and norepinephrine

Ying Li, Yogeswaran Umasankar, Shen-Ming Chen *

Department of Chemical Engineering and Biotechnology, National Taipei University of Technology, No. 1, Section 3, Chung-Hsiao East Road, Taipei 106, Taiwan, ROC

ARTICLE INFO

Article history:
Received 22 December 2008
Available online 1 March 2009

Keywords:
Multiwall carbon nanotubes
Biocomposite film
Modified electrodes
Electrocatalysis
Epinephrine
Norepinephrine

ABSTRACT

A novel biocomposite film (MWCNTs–P*NDGAChi*), which contains multiwalled carbon nanotubes (MWCNTs) along with the incorporation of poly(nordihydroguaiaretic acid) and chitosan copolymer (P*NDGAChi*), has been synthesized on gold electrode by potentiostatic methods. The presence of MWCNTs in the biocomposite film enhances P*NDGAChi*'s surface coverage concentration (Γ) on the electrode and decreases degradation of P*NDGAChi* during cycling. The biocomposite film also exhibits promising enhanced electrocatalytic activity toward the oxidation of biochemical compounds such as epinephrine (EP) and norepinephrine (NEP). Cyclic voltammetry was used for the measurement of electroanalytical properties of analytes by means of MWCNTs–P*NDGAChi* biocomposite film modified gold electrode. The sensitivity values of MWCNTs–P*NDGAChi* biocomposite film modified gold electrode are higher than the values obtained for P*NDGAChi* film modified gold electrode. Electrochemical quartz crystal microbalance studies reveal the enhancements in the functional properties of MWCNTs and P*NDGAChi* present in MWCNTs–P*NDGAChi* biocomposite film. Surface morphology of the biocomposite films was studied using scanning electron microscopy, atomic force microscopy, and scanning tunneling microscopy. The surface morphology results reveal that P*NDGAChi* incorporated on MWCNTs. Finally, flow injection analysis was used for the amperometric detection of EP and NEP at MWCNTs–P*NDGAChi* film modified screen printed carbon electrode.

Electropolymerization is a simple but powerful method in targeting selective modification of different types of electrodes with desired matrices. However, the materials on the matrices do not possess peculiar properties when compared with those materials that are chemically synthesized by traditional methods. The electroactive polymers and carbon nanotubes (CNTs)[1] matrices have received considerable attraction during recent years. Numerous conjugated polymers have been electrochemically synthesized for their application in the fabrication of chemical and biochemical sensor devices [1]. These conjugated polymers for sensor devices exhibit interesting enhancement in the electrocatalytic activity toward the oxidation or reduction of several biochemical and inorganic compounds [2] where some of the functional groups in polymers will act as catalyst [3–5]. In this article, the term "enhanced electrocatalytic activity" could be described as both increase in peak current and lower overpotential [6]. The wide variety of applications of matrices made of CNTs for the detection of inorganic and bioorganic compounds such as IO_3^- and ascorbic acid have already been reported in the literature [7–9]. Even though the electrocatalytic activity of conjugated polymers and CNTs matrices individually shows good results, some properties such as mechanical stability, sensitivity for different techniques, and electrocatalysis for multiple compound detections are found to be poor. To overcome this difficulty, new studies have been developed during the past decade for the preparation of composite films composed of both CNTs and conjugated polymers. The rolled-up graphene sheets of carbon exhibit π-conjugative structure with highly hydrophobic surface. This unique property of the CNTs allows them to interact with organic aromatic compounds through π–π electronic and hydrophobic interactions to form new structures [10,11]. There were past attempts in the preparation of composite and sandwiched films made of polymer adsorbed on CNTs, and these were used for electrocatalytic studies such as selective detection of dopamine in the presence of ascorbic acid [12]. The sandwiched films were also used in the designing of nanodevices with the help of noncovalent adsorption, electrodeposition, and the like [13].

Biopolymer chitosan (*Chi*) is a polysaccharide derived by deacetylation of chitin. It has primary amino groups that have a

* Corresponding author. Fax: +886 2270 25238.
E-mail address: smchen78@ms15.hinet.net (S.-M. Chen).

[1] *Abbreviations used:* CNT, carbon nanotube; *Chi*, chitosan; NDGA, nordihydroguaiaretic acid; P*NDGA*, poly-*NDGA*; EP, epinephrine; NEP, norepinephrine; MWCNT, multiwalled carbon nanotube; PBS, phosphate buffer solution; EQCM, electrochemical quartz crystal microbalance; FIA, flow injection analysis; SPCE, screen-printed carbon electrode; SEM, scanning electron microscopy; AFM, atomic force microscopy; STM, scanning tunneling microscopy; CV, cyclic voltammogram.

0003-2697/$ - see front matter © 2009 Elsevier Inc. All rights reserved.
doi:10.1016/j.ab.2009.02.032

pK_a value of approximately 6.3 [14]. Due to the presence of abundant primary amino groups, *Chi* possesses many advantages such as excellent membrane-forming ability, high permeability toward water, good adhesion, biocompatibility, nontoxicity, high mechanical strength, and susceptibility to chemical modification [15]. On the other hand, different nonmetallic redox polymers exhibit excellent catalytic properties toward the electrochemical oxidation of biologically important analytes and have found successful applications in the development of biosensors. Nordihydroguaiaretic acid (NDGA, 1,4-bis-(3,4-dihydroxyphenyl)-2,3-dimethylbutane)) is one such naturally occurring antioxidant found in *Larrea tridentate* [16]. Being a catechol derivative, it is electrochemically active and undergoes characteristic $2e/2H^+$ transition. When it is oxidized electrochemically, it forms highly active polymeric film (P*NDGA*) on the electrode surface [17].

Epinephrine (EP) and norepinephrine (NEP) are important catecholamine neurotransmitters in the mammalian central nervous system, which plays an important role in the function of the central nervous, renal, hormonal, and cardiovascular systems. The catecholamine drugs are used to treat hypertension, bronchial asthma, and organic heart disease and are used in cardiac surgery and myocardial infarction [18,19]. The oxidation of these compounds is interesting as this process occurs in the human body. Due to their crucial role in neurochemistry and industrial applications, several traditional methods have been used for their determination. Among these, the electrochemical methods have more advantages over the others in sensing neurotransmitters present in living organisms.

The literature survey reveals that there are no previous attempts made for the synthesis of biocomposite film composed of CNTs, P*NDGA,* and *Chi* for the use in sensor applications. In this article, we report on a novel composite film (MWCNTs–P*NDGAChi*) made of multiwalled carbon nanotubes (MWCNTs) which is incorporated with P*NDGAChi* copolymer. MWCNTs–P*NDGAChi* biocomposite film's characterization, enhancement in functional properties, stability, peak current, and electrocatalytic activity have also been reported along with its application in the determination of EP and NEP. The film formation processing involves the modification of gold electrode with uniformly well-dispersed MWCNTs, which is then modified with P*NDGAChi* copolymer.

Materials and methods

Materials

NDGA, *Chi,* MWCNTs (o.d. = 10–20 nm, i.d. = 2–10 nm, length = 0.5–200 μm), potassium hydroxide, EP, and NEP were obtained from Aldrich and Sigma–Aldrich and were used as received. All other chemicals used were of analytical grade. The preparation of aqueous solution was done with double distilled deionized water. Solutions were deoxygenated by purging with prepurified nitrogen gas. Buffer solutions were prepared from H_2SO_4 and 1% acetic acid for the pH 2.18 aqueous solution and with phosphate buffer (0.1 M Na_2HPO_4 and 0.1 M NaH_2PO_4) for the pH 7.0 aqueous solution (PBS).

Apparatus

Cyclic voltammetry experiments were performed in analytical systems model CHI-611, CHI-400, and CHI-1205A potentiostats. A conventional three-electrode cell assembly consisting of Ag/AgCl reference electrode and a Pt wire counter electrode were used for the electrochemical measurements. The working electrodes are either an unmodified gold or gold modified with P*NDGA,* MWCNTs–P*NDGA,* or MWCNTs–P*NDGAChi* biocomposite films. In these experiments, all of the potentials are reported versus Ag/AgCl reference electrode. The working electrode used for electrochemical quartz crystal microbalance (EQCM) measurements was an 8-MHz AT-cut quartz crystal coated with gold electrode. The diameter of the quartz crystal is 13.7 mm, and the diameter of the gold electrode is 5.0 mm. The flow injection analysis (FIA) of the analytes at screen-printed carbon electrode (SPCE) was done using an Alltech 426 HPLC pump containing an electrochemical cell. The surface morphology characterizations of the films were examined by means of scanning electron microscopy (SEM, Hitachi S-3000H), atomic force microscopy (AFM), and scanning tunneling microscopy (STM, Being Nano-Instruments, model CSPM4000). All of the measurements were carried out at 25 ± 2 °C.

Preparation of MWCNTs dispersion and MWCNTs–PNDGAChi modified electrode

There was an important challenge in the dispersion of MWCNTs. Because of their hydrophobic nature, it was difficult to disperse them in any aqueous solution to get a homogeneous mixture. Briefly, the hydrophobic nature of the MWCNTs was converted into a hydrophilic nature by following the previous studies [20,21]. Briefly, this was done by adding 10 mg of MWCNTs and 200 mg of potassium hydroxide into a ruby mortar and graining together for 2 h at room temperature. Then the reaction mixture was dissolved in 10 ml of double distilled deionized water, and it was precipitated many times into methanol for the removal of potassium hydroxide. MWCNTs obtained in 10 ml of water were ultrasonicated for 6 h to get a uniform dispersion. This functionalization process of MWCNTs was done to get the hydrophilic nature for the homogeneous dispersion in water. This process not only converts MWCNTs to a hydrophilic nature but also helps to break down larger bundles of MWCNTs into smaller ones. This process was confirmed using SEM.

Before starting each experiment, the gold electrodes were polished by a BAS polishing kit with a 0.05-μm alumina slurry, rinsed, and then ultrasonicated in double distilled deionized water. The gold electrodes studied were uniformly coated with 50 μg cm^{-2} MWCNTs and then dried at 35 °C. The concentrations of homogeneously dispersed MWCNTs were measured exactly using a microsyringe. The electropolymerization of NDGA and *Chi* to form P*NDGAChi* copolymer was performed from the mixture of 0.5 mM NDGA and 0.5 mM *Chi* present in pH 2.18 aqueous solution by consecutive cyclic voltammograms (CVs) over a suitable potential region of −0.8 to 0.8 V. Then the modified MWCNTs–P*NDGAChi* electrode was carefully washed with double distilled deionized water. The mixture of NDGA and *Chi* solution was prepared by mixing 1:1 ratio of NDGA (0.5 mM) present in H_2SO_4 (pH 1.0) with *Chi* (0.5 mM) present in 1% acetic acid. For a detailed comparison of electrocatalysis reactions, different types of modified electrodes were studied: P*NDGA,* MWCNTs–P*NDGA,* and MWCNTs–P*NDGAChi.* These comparison studies were done to reveal the obvious necessity of the presence of MWCNTs in MWCNTs–P*NDGAChi* biocomposite film.

For AFM studies, the tapping mode with scan scope, scan rate, and set point of 10 μm, 0.8 Hz, and 0.65, respectively, were used. Similarly for STM studies, the bias and set point were 0.05 V and 1.0, respectively. In addition, the scan rates for bare gold, P*NDGAChi,* and MWCNTs–P*NDGAChi* were 2.0, 1.0, and 0.4 Hz, respectively. For EP and NEP electrocatalysis experiments, the film modified electrodes were washed carefully in deionized water and transferred to PBS (pH 7.0), and then the CVs were recorded at a constant time interval of 1 min with nitrogen purging before the start of each experiment. For FIA, the carrier stream used was PBS with a flow rate of 3.5 ml min^{-1}, and the volume of analytes injected at each cycle was 10 μl at a time interval of 50 s.

Results and discussions

Electrochemical synthesis of MWCNTs–PNDGAChi biocomposite film and its characterization

The electropolymerization of NDGA (0.5 mM) with *Chi* (0.5 mM) mixture on MWCNTs modified gold electrode present in pH 2.18 aqueous solution was performed by consecutive CVs for the preparation of MWCNTs–P*NDGAChi* biocomposite film. Fig. 1A shows the reduction and electropolymerization of NDGA with *Chi* at MWCNTs modified gold electrode. A redox peak ($E^{0'}$ = 458 mV) has been obtained for P*NDGAChi* during electropolymerization, which represents the electrochemical redox reaction of P*NDGAChi* copolymer present in MWCNTs–P*NDGAChi* biocomposite film.

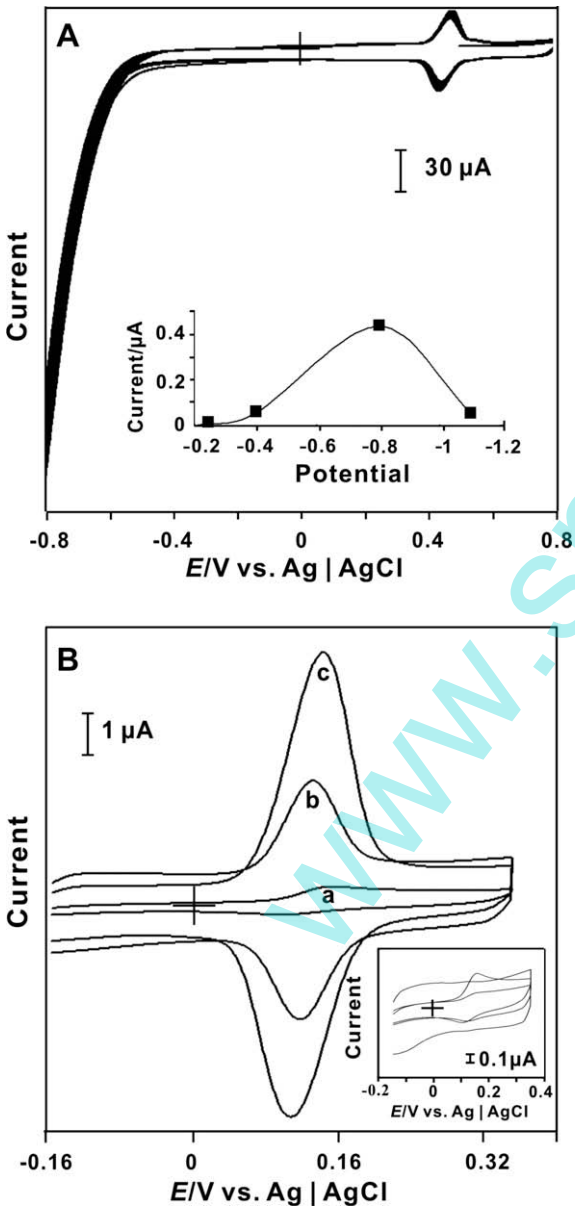

Fig. 1. (A) Repetitive CVs of MWCNTs–gold electrode modified from 0.5 mM NDGA with 0.5 mM *Chi* present in pH 2.18 aqueous solution (scan rate = 100 mV s^{-1}). The inset shows NDGA polymerization at different potentials versus P*NDGA* peak current. (B) Comparison of CVs of P*NDGA* (a), MWCNTs–P*NDGA* (b), and MWCNTs–P*NDGAChi* (c) biocomposite films at gold electrode in pH 7.0 PBS (scan rate = 20 mV s^{-1}). The inset shows only MWCNTs, P*NDGAChi*, and MWCNTs–*Chi* redox peak currents at gold electrode in PBS (scan rate = 20 mV s^{-1}).

The increase in peak current of the same redox couple at each cycle reveals the continuous deposition of P*NDGAChi* during cycling. The electropolymerization was carried out at a suitable potential range of −0.8 to 0.8 V. This suitable potential range was optimized using the plots given in the Fig. 1A inset; these were plotted based on the electropolymerization of NDGA along with *Chi* at different reduction potentials ranging from −0.2 to −1.1 V. Briefly, the polymerized NDGA along with *Chi* at each potential was carefully washed in deionized water to remove the NDGA and *Chi* adsorbed on gold electrode. Then the modified gold electrodes were transferred to pH 2.18 aqueous solution in the absence of NDGA and *Chi* for CV characterization, from which the I_{pa} plots were obtained and are given in the Fig. 1A inset. These CV results show that an increasing anodic peak current of the redox couple occurred if the reduction potential was from −0.2 to −0.8 V. However, there was a sudden decrease in the redox peak currents if the reduction potential for electropolymerization was above −0.8 V. This result shows the removal of P*NDGAChi* from the gold electrode at higher negative potentials. In the following experiments, each newly prepared MWCNTs–P*NDGAChi* biocomposite film on gold electrode was washed carefully in deionized water to remove the loosely bound NDGA and *Chi* on the modified gold electrode. It was then transferred to pH 7.0 PBS for other electrochemical characterizations. These optimized pH solutions were chosen to maintain the higher stability of the biocomposite film.

Fig. 1B represents the electrochemical signal of P*NDGA* redox reaction with the formal potential $E^{0'}$ = 0.14 mV versus Ag/AgCl in PBS (scan rate = 20 mV s^{-1}) in bare gold electrode (voltammogram a) and MWCNTs modified gold electrode (voltammogram b), whereas voltammogram c shows higher peak current for MWCNTs–P*NDGAChi* modified gold electrode. The above result shows that the formation of P*NDGAChi* copolymer in voltammogram c enhances the redox peak current of P*NDGA*. This reveals that in voltammogram c both MWCNTs and *Chi* play vital roles in enhancing the peak current of P*NDGA*. From the CVs in Fig. 1B, the surface coverage concentration (Γ) values were calculated and are given in Table 1. In this calculation, the charge involved in the reaction (Q) was obtained from CVs and applied in the equation $\Gamma = Q/nFA$, where the number of electron transfers involved in the P*NDGAChi* redox reaction is assumed to be two. These values indicate that the presence of MWCNTs increases the surface area of the electrode, which in turn increases Γ of P*NDGA*. Furthermore, the presence of *Chi* in the film enhances the peak current of P*NDGA*. The Fig. 1B inset shows that there are no redox peak currents for only MWCNTs, MWCNTs–P*Chi*, or P*NDGAChi*.

The CVs of MWCNTs–P*NDGAChi* biocomposite film on gold electrode in pH 7.0 PBS at different scan rates demonstrate that the redox process is not controlled by diffusion. Further investigation revealed that the separation between anodic (I_{pa}) and cathodic (I_{pc}) peak currents for all three films increased as the scan rate increased, as shown in Fig. 2A. From the slope values between ΔE_p versus log scan rate (not shown), by assuming the value of $\alpha \sim 0.50$, the electron transfer rate constant (k_s) was calculated based on Laviron theory [22] and $k_s \sim 0.57$ s^{-1} for MWCNTs–P*NDGAChi* biocomposite film. Fig. 2B shows the CVs of MWCNTs–P*NDGAChi* on gold electrode at various pH aqueous solutions in which the NDGA and *Chi* are absent. In these experiments, the MWCNTs

Table 1
Surface coverage concentration (Γ) of P*NDGA* at various gold modified electrodes.

Electrode type	Modified film	Γ (pmol cm^{-2})
Au[a]	P*NDGA*	7.23
	MWCNTs–P*NDGA*	187
	MWCNTs–P*NDGAChi*	432

[a] Studied using CV technique in PBS (pH 7.0).

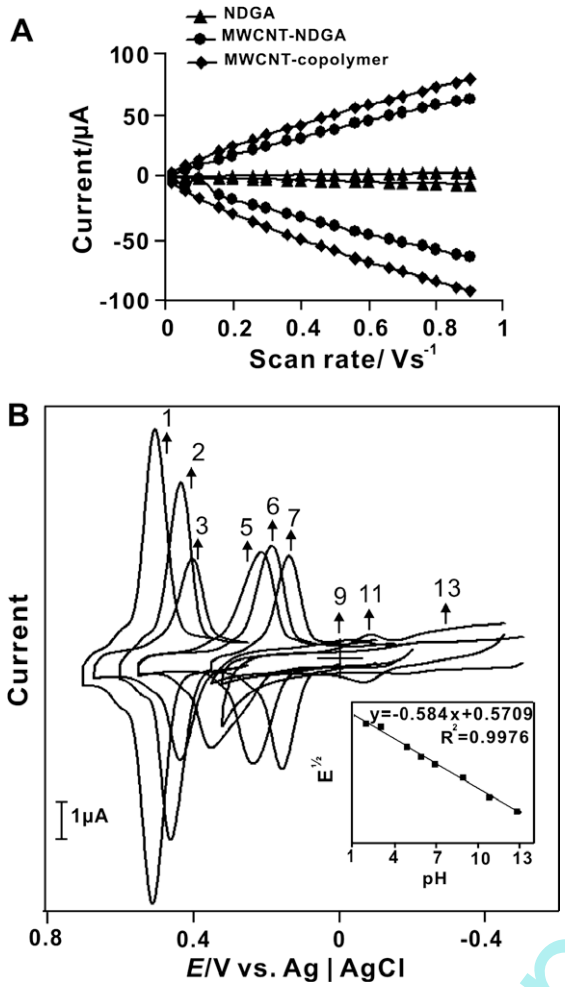

Fig. 2. (A) Plots of I_{pa} and I_{pc} versus different scan rates for P*NDGA*, MWCNTs–P*NDGA*, and MWCNTs–P*NDGAChi* biocomposite films present in PBS. (B) CVs of MWCNTs–P*NDGAChi* biocomposite film synthesized at pH 2.18 on gold electrode and transferred to various pH solutions. The inset shows formal potential versus pH.

coated gold electrode was modified with P*NDGAChi* using pH 2.18 aqueous solution, washed with deionized water, and then transferred to various pH aqueous solutions for CV measurements. These CV results show that the film was stable in the pH range between 1.0 and 13.0 and that the E_{pa} and E_{pc} values depend on the pH value of the aqueous solution. The Fig. 2B inset shows the formal potential of MWCNTs–P*NDGAChi* redox couple plotted over the pH range of 1.0 to 13.0. The response shows a slope of −58 mV pH^{-1}, which is close to that given by the Nernstian equation for an equal number of electrons and protons transfer [23,24].

EQCM and morphology characterization of MWCNTs–PNDGAChi biocomposite film

The EQCM experiments were carried out by modifying the gold in electrochemical quartz crystal, uniformly coated with and without MWCNTs, which was then dried at 35 °C. From the frequency change, change in the mass of biocomposite film at quartz crystal was calculated by using the Sauerbrey equation. From this calculation for the above-mentioned experimental conditions, it was found that a 1-Hz frequency change is equal to 1.4 ng of mass change [25–28]. Therefore, mass changes during P*NDGAChi* incorporation on the modified and unmodified MWCNTs gold electrodes for total cycles were 284 and 210 ng cm^{-2}, respectively, consistent with the Γ values of P*NDGA*. Fig. 3A and B represents the presence and absence of MWCNTs, respectively, on the gold electrode, whereas voltammograms a and b indicate cycle frequency change with the increase of the scan cycles and variation of frequency change with the increase of scan cycles, respectively. From these plots, it is clear that there is an unstable deposition of P*NDGAChi* in the absence of MWCNTs. This proves that the deposition of P*NDGAChi* on MWCNTs film is more stable and more homogeneous than that on bare gold electrode. Similar previous studies on CNTs biocomposite have also shown the necessity of CNTs for improving the functional properties such as orientation, enhanced electron transport, and high capacitance [29,30].

Furthermore, three different films—MWCNTs, P*NDGAChi*, and MWCNTs–P*NDGAChi*—were prepared on gold electrode with similar conditions and similar potential and were characterized using SEM. It is a well-known fact that the prolonged exposure to electron beam will damage the P*NDGAChi* films, so a great deal of care was taken to measure these images. Comparison of Fig. 4A and B reveals a significant morphological difference between P*NDGAChi* and MWCNTs–P*NDGAChi* films. The top views of nanostructures in Fig. 4A on the gold electrode surface show white patches of P*NDGAChi* deposited on this electrode. The MWCNTs–P*NDGAChi* biocomposite film in Fig. 4B shows that the P*NDGAChi* covered the entire MWCNTs to form MWCNTs–P*NDGAChi* biocomposite modified gold electrode. Similarly, a′ and b′ represent bare gold electrode and only MWCNTs, respectively. The same modified gold electrodes were used to measure the AFM topography images shown in Fig. 5A (P*NDGAChi*) and Fig. 5B (MWCNTs–P*NDGAChi*), where a′ is the bare gold electrode. The higher magnification (10 × 10 μm) of AFM images when comparing SEM images reveals that elongated grain-shaped structures of P*NDGAChi* formed on the gold electrode. However, in Fig. 5B, huge platelet structures of P*NDGAChi* formed instead of an elongated grain shape. This result reveals that a higher concentration of P*NDGAChi* was deposited on MWCNTs modified gold electrode, consistent with the Γ values

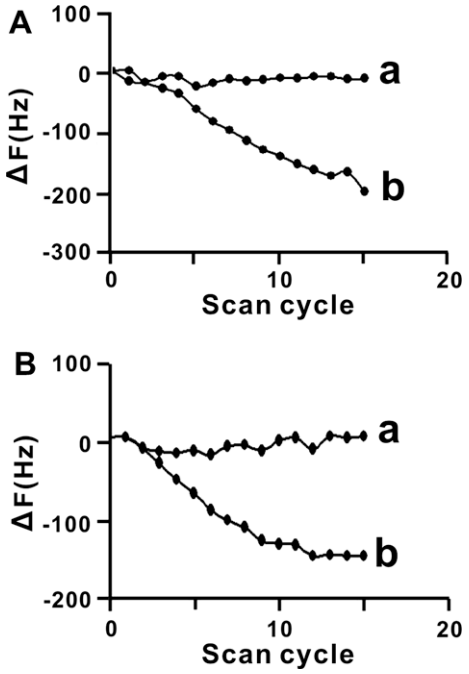

Fig. 3. Consecutive potential CVs of a gold electrode modified with P*NDGAChi* at 0.8 V to −0.8 V (scan rate = 20 mV s^{-1}), where panels (A and B) show the presence and absence of MWCNTs on the gold electrode. In both panels, voltammograms a and b indicate cycle frequency change with the increase of the scan cycles and variation of frequency change with the increase of scan cycles, respectively.

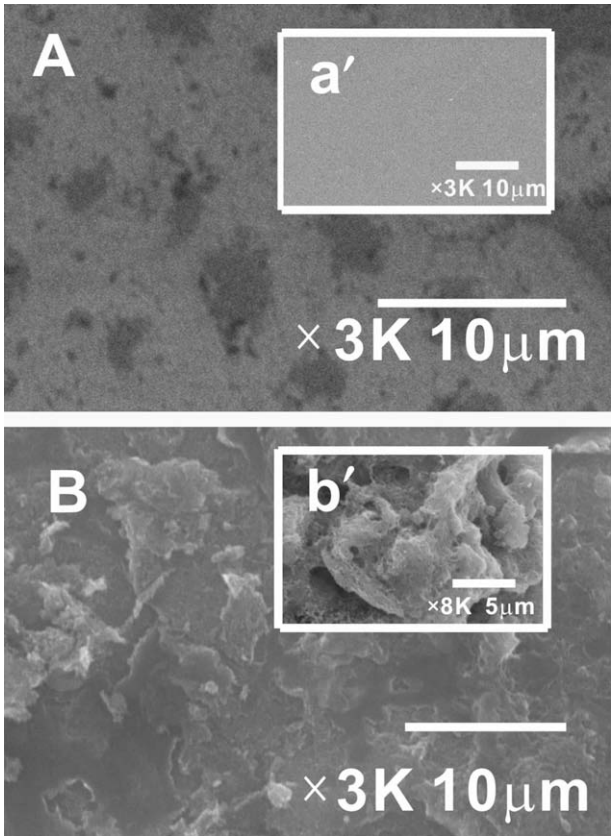

Fig. 4. SEM images of P*NDGAChi* (A) and MWCNTs–P*NDGAChi* (B) biocomposite films, where a′ is bare gold electrode and b′ is only MWCNTs.

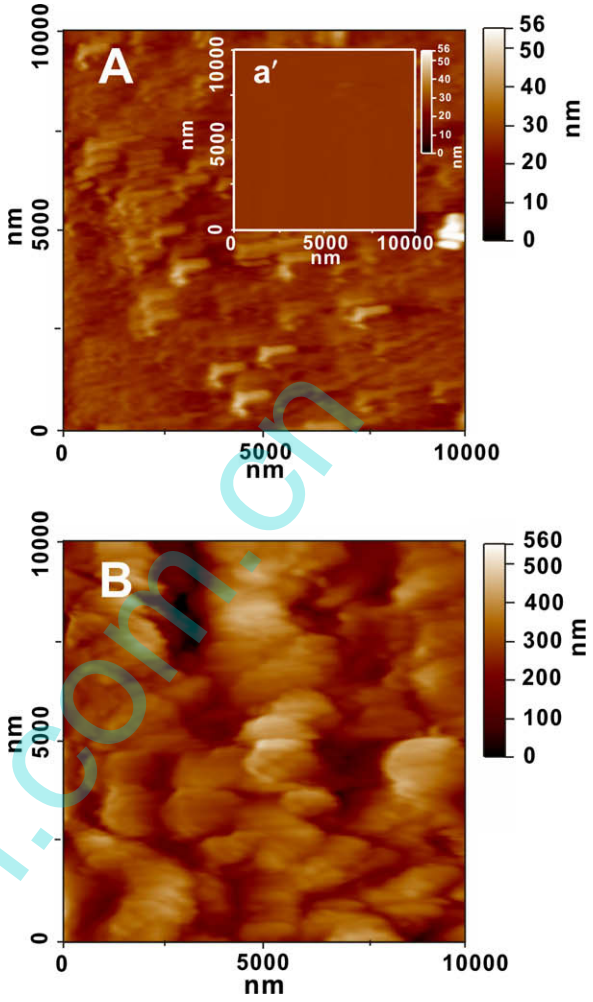

Fig. 5. AFM images of P*NDGAChi* (A) and MWCNTs–P*NDGAChi* (B) biocomposite films, where a′ is bare gold electrode.

shown in Table 1. Furthermore, the thicknesses of P*NDGAChi* and MWCNTs–P*NDGAChi* obtained from AFM results were 56 and 560 nm, respectively. These values also show that MWCNTs–P*NDGAChi* is thicker than P*NDGAChi* due to the presence of MWCNTs covered under P*NDGAChi* film. Similarly, STM images were also measured for P*NDGAChi* (Fig. 6A), MWCNTs–P*NDGAChi* (Fig. 6B), and bare gold electrode (a′). These STM images are much more magnified than AFM images (shown on a scale of 200 × 200 nm). The coexistence of MWCNTs and P*NDGAChi* clearly revealed in Fig. 6B where each huge platelet structures of P*NDGAChi* was covered over MWCNTs. All of these SEM, AFM, and STM results reveal the coexistence of MWCNTs and P*NDGAChi* in the biocomposite film.

Electroanalytical response of EP and NEP at MWCNTs–PNDGAChi biocomposite film

The MWCNTs–P*NDGAChi* biocomposite film was synthesized on gold electrode at similar conditions as described in Materials and Methods. Then the biocomposite film modified electrode was washed carefully in deionized water and transferred to PBS for the electrocatalysis of EP and NEP. The pH of the PBS solution was 7.0, where the biocompounds were stable. All of the CVs were recorded at the constant time interval of 1 min with nitrogen purging before the start of each experiment. Fig. 7A and B shows the electrocatalytic oxidation of EP and NEP, respectively, at various biocomposite films with a scan rate of 20 mV s^{-1}. In all of the sections of Fig. 7, a′ represents bare gold electrode, voltammogram a is the P*NDGAChi,* voltammogram b is MWCNTs at the highest concentrations of EP (1.28 mM) and NEP (31.80 mM), and voltammograms c to g represent different concentrations of EP (0 and 0.03–1.28 mM) and NEP (0 and 0.78–31.80 mM) at MWCNTs–P*NDGAChi*. The CVs for MWCNTs–P*NDGAChi* exhibit a reversible redox couple in the absence of EP and NEP, and on the addition of analytes a new growth in the oxidation peak of analytes appeared at E_{pa} = 0.18 V for EP (Fig. 7A) and E_{pa} = 0.25 V for NEP (Fig. 7B). These peak currents show that electrocatalytic oxidation of both the analytes takes place at P*NDGA* redox couple.

In these above electrocatalysis experiments, an increase in concentration c to g of EP (Fig. 7A) and NEP (Fig. 7B) simultaneously produces a linear increase in the oxidation peak currents of the respective analytes with good film stability at MWCNTs and MWCNTs–P*NDGAChi* films. However, there was no increase at P*NDGAChi* film and bare gold electrode. The anodic peak currents are linear with the concentration of EP and NEP. It is obvious that the MWCNTs–P*NDGAChi* shows higher electrocatalytic activity for both EP and NEP. More specifically, the enhanced electrocatalysis of MWCNTs–P*NDGAChi* can be explained in terms of higher peak current than that of MWCNTs film and both lower overpotential and higher peak current than that of P*NDGAChi* film. These results can be observed from the I_{pa} and E_{pa} values given in Table 2, where the increase in peak current and lower overpotential both are considered as the electrocatalysis [6]. From the slopes of linear calibration curves, the sensitivities of MWCNTs and MWCNTs–P*NDGAChi* biocomposite film modified gold electrodes and their correlation coefficient were calculated and are given in Table 3. It is obvious that the sensitivity of MWCNTs–P*NDGAChi* film is higher for both

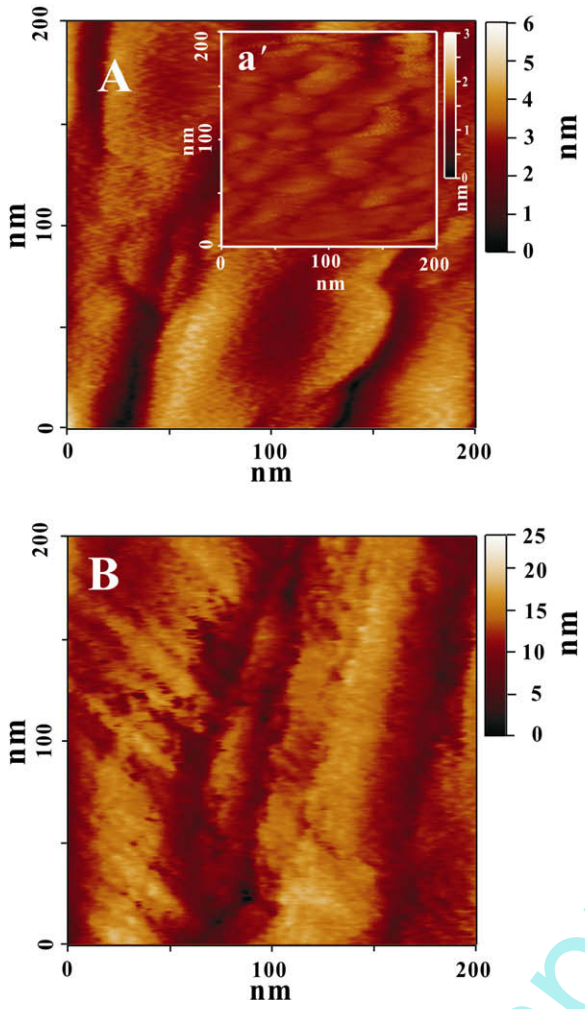

Fig. 6. STM images of P*NDGAChi* (A) and MWCNTs–P*NDGAChi* (B) biocomposite films, where a′ is bare gold electrode.

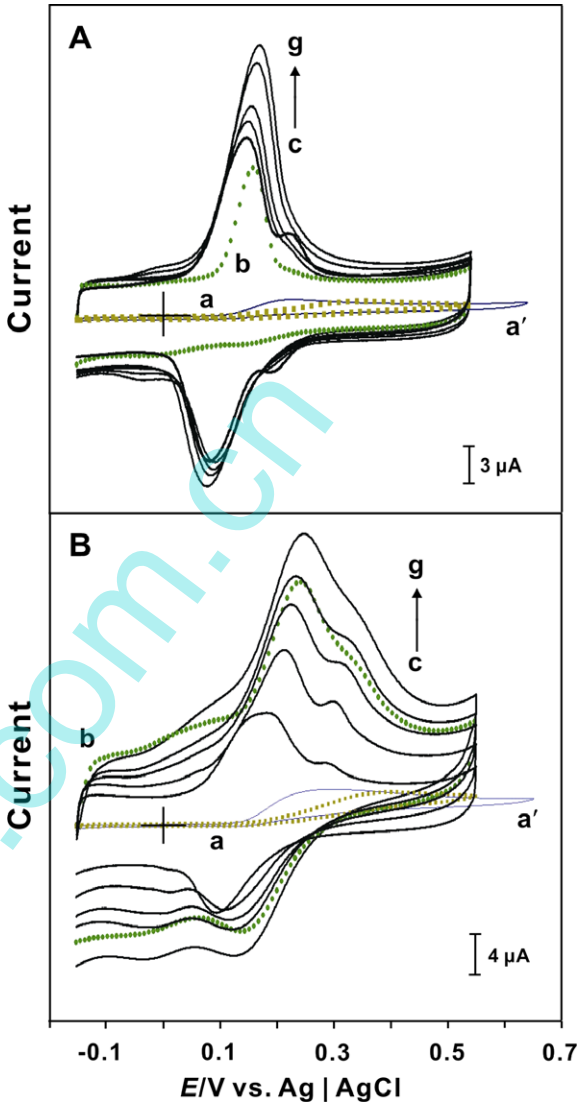

Fig. 7. CVs of EP (A) and NEP (B) at various electrodes using pH 7.4 PBS at 20 mV s^{-1}, where a′ is at bare gold electrode, voltammogram a is at P*NDGAChi*, and voltammogram b is at MWCNTs–P*NDGA* in a higher concentration of analytes (EP = 1.28 mM, NEP = 31.80 mM). Voltammograms c to g in panel (A): [EP] = 0.0 mM (c), 0.03 mM (d), 0.28 mM (e), 0.78 mM (f), and 1.28 mM (g) at MWCNTs–P*NDGAChi*. Voltammograms c to g in panel (B): [NEP] = 0.0 mM (c), 0.78 mM (d), 1.28 mM (e), 1.98 mM (f), and 31.8 mM (g) at MWCNTs–P*NDGAChi*.

analytes when compared with MWCNTs film. The overall view of these results clearly reveals that MWCNTs–P*NDGAChi* biocomposite film is efficient for EP and NEP detection.

FIA of EP and NEP at MWCNTs–PNDGAChi biocomposite film

The MWCNTs–P*NDGAChi* biocomposite film was synthesized on SPCE at similar conditions to that of gold electrode. Then the modified electrode was washed carefully in deionized water and used for FIA of EP and NEP as shown in Fig. 8A and B, respectively. The carrier stream used was pH 7.0 PBS with a flow rate of 3.5 ml min^{-1}, and the volume of analytes injected at each cycle was 10 μl at a time interval of 50 s. Both Fig. 8A and B are the successive additions of EP and NEP in the concentration range from 0.1 mM to 0.1 M at the potentials of 172 mV for EP and 244 mV for NEP. These potentials are the optimized potentials obtained from CV studies. The rapid amperometric response of the MWCNTs and MWCNTs–P*NDGAChi* biocomposite film is proportional to the respective analyte concentration. From the slopes of linear calibration curves, sensitivities of MWCNTs and MWCNTs–P*NDGAChi* biocomposite film modified SPCE and their correlation coefficient were calculated and are given in Table 3. The comparison of slope values of both the films shows that the MWCNTs–P*NDGAChi* biocomposite film possesses good reproducibility with higher sensitivity for both of the analytes.

Table 2
Comparison of E_{pa} and I_{pa} of analytes in electrocatalysis reactions using CV technique at different type modified electrodes in PBS.

Analyte	Reaction type	pH	E_p (V)			I_p (μA)		
			P*NDGAChi*	MWCNTs	MWCNTs–P*NDGAChi*	P*NDGAChi*	MWCNTs	MWCNTs–P*NDGAChi*
EP	Oxidation	7.0	0.35	0.161	0.172	1.067	7.950	15.53
NEP	Oxidation	7.0	0.396	0.238	0.244	3.045	12.11	15.01

Table 3
Sensitivities and correlation coefficients of different modified electrodes for various analytes in different techniques.

Technique	Analyte	Reaction type	Sensitivity ($\mu A\ \mu M^{-1}\ cm^{-2}$) and correlation coefficient	
			MWCNTs	MWCNTs–P*NDGAChi*
Cyclic voltammetry	EP	Oxidation	1154 (0.9282)	1964 (0.9828)
	NEP	Oxidation	1076.5 (0.9639)	3067 (0.9914)
FIA	EP	Oxidation	126 (0.7444)	204 (0.782)
	NEP	Oxidation	267 (0.8321)	457 (0.8962)

Note. Correlation coefficients are in parentheses.

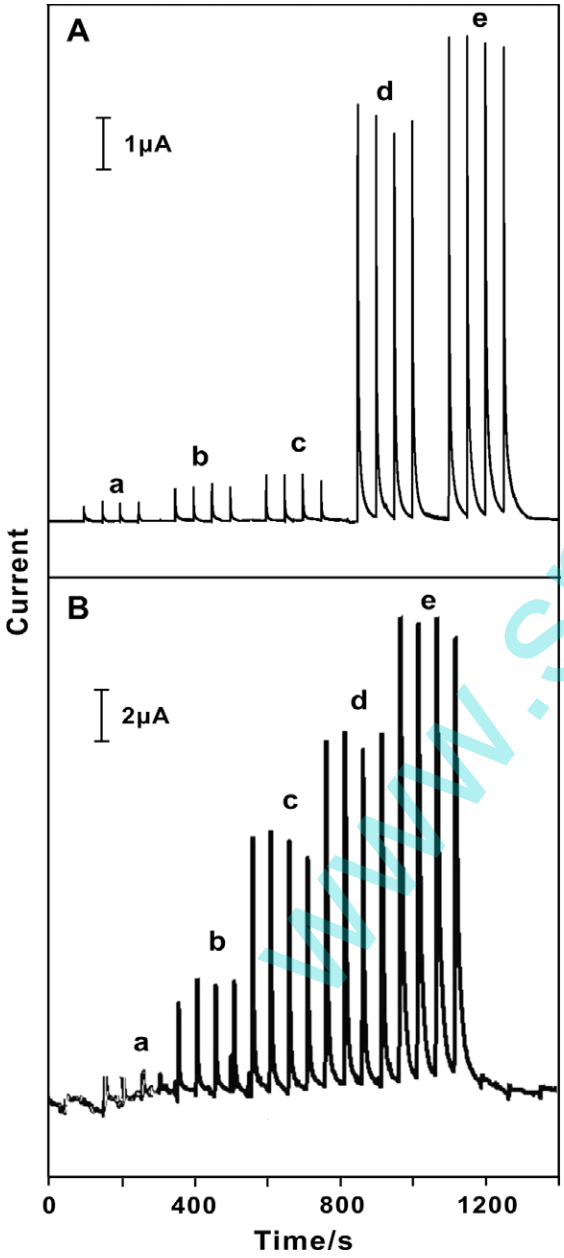

Fig. 8. (A) FIA of EP at MWCNTs–P*NDGAChi* biocomposite film present in PBS with five different concentrations of [EP] = 1×10^{-4} M (a), 8×10^{-4} M (b), 4×10^{-3} M (c), 1×10^{-2} M (d), and 1×10^{-1} M (e), where potential = 172 mV. (B)) FIA of NEP at MWCNTs–P*NDGAChi* biocomposite film present in PBS with five different concentrations of [NEP] = 1×10^{-4} M (a), 8×10^{-4} M (b), 4×10^{-3} M (c), 1×10^{-2} M (d), and 1×10^{-1} M (e), where potential = 244 mV. In all three of these experiments, the carrier stream used was PBS, flow rate = 3.5 ml min^{-1}, and injected volume = 10 μl.

Conclusions

We have developed a novel biocomposite material using MWCNTs, P*NDGA*, and P*Chi* (MWCNTs–P*NDGAChi*) at gold and SPCE electrode surfaces, which are more stable in PBS. The developed biocomposite film for the electrocatalysis combines the advantages of ease of fabrication, high reproducibility, and sufficient long-term stability. The EQCM result confirmed the incorporation of P*NDGAChi* on MWCNTs modified gold electrode. The SEM, AFM, and STM results showed the difference between P*NDGAChi* and MWCNTs–P*NDGAChi* biocomposite films morphology. Furthermore, it was found that the MWCNTs–P*NDGAChi* biocomposite film has excellent functional properties along with good electrocatalytic activity on EP and NEP. The experimental methods of CV and FIA with biocomposite film biosensor integrated into the gold electrode and SPCE, as presented in this article, provide an opportunity for qualitative and quantitative characterization. Therefore, this work establishes and illustrates in principle and potential a simple and novel approach for the development of a voltammetric and amperometric sensor that is based on modified gold electrode and SPCE.

Acknowledgment

This work was supported by the National Science Council and the Ministry of Education of Taiwan (Republic of China).

References

[1] C.P. McMahon, G. Rocchitta, S.M. Kirwan, S.J. Killoran, P.A. Serra, J.P. Lowry, R.D. O'Neill, Oxygen tolerance of an implantable polymer/enzyme composite glutamate biosensor displaying polycation-enhanced substrate sensitivity, Biosens. Bioelectron. 22 (2007) 1466–1473.
[2] I. Becerik, F. Kadirgan, Glucose sensitivity of platinum-based alloys incorporated in polypyrrole films at neutral media, Synthetic Metals 124 (2001) 379–384.
[3] T. Selvaraju, R.R. Ramaraj, Electrochemically deposited nanostructured platinum on Nafion coated electrode for sensor applications, J. Electroanal. Chem. 585 (2005) 290–300.
[4] M. Mao, D. Zhang, T. Sotomura, K. Nakatsu, N. Koshiba, T. Ohsaka, Mechanistic study of the reduction of oxygen in air electrode with manganese oxides as electrocatalysts, Electrochim. Acta 48 (2003) 1015–1021.
[5] M. Yasuzawa, A. Kunugi, Properties of glucose sensors prepared by the electropolymerization of a positively charged pyrrole derivative, Electrochem. Commun. 1 (1999) 459–462.
[6] C.P. Andrieux, O. Haas, J.M. SavGant, Catalysis of electrochemical reactions at redox-polymer-coated electrodes: mediation of the iron(III)/iron(II) oxido-reduction by a polyvinylpyridine polymer containing coordinatively attached bisbipyridine chlororuthenium redox centers, J. Am. Chem. Soc. 108 (1986) 8175–8182.
[7] J. Wang, M. Musameh, Electrochemical detection of trace insulin at carbon-nanotube-modified electrodes, Anal. Chim. Acta 511 (2004) 33–36.
[8] H. Cai, X. Cao, Y. Jiang, P. He, Y. Fang, Carbon nanotube-enhanced electrochemical DNA biosensor for DNA hybridization detection, Anal. Bioanal. Chem. 375 (2003) 287–293.
[9] A. Erdem, P. Papakonstantinou, H. Murphy, Direct DNA hybridization at disposable graphite electrodes modified with carbon nanotubes, Anal. Chem. 78 (2006) 6656–6659.
[10] Q. Li, J. Zhang, H. Yan, M. He, Z. Liu, Thionine-mediated chemistry of carbon nanotubes, Carbon 42 (2004) 287–291.
[11] J. Zhang, J.K. Lee, Y. Wu, R.W. Murray, Photoluminescence and electronic interaction of anthracene derivatives adsorbed on sidewalls of single-walled carbon nanotubes, Nano Lett. 3 (2003) 403–407.
[12] M. Zhang, K. Gong, H. Zhang, L. Mao, Layer-by-layer assembled carbon nanotubes for selective determination of dopamine in the presence of ascorbic acid, Biosens. Bioelectron. 20 (2005) 1270–1276.
[13] R.J. Chen, Y. Zhang, D. Wang, H. Dai, Noncovalent sidewall functionalization of single-walled carbon nanotubes for protein immobilization, J. Am. Chem. Soc. 123 (2001) 3838–3839.
[14] P. Sorlier, A. Denuzière, C. Viton, A. Domard, Relation between the degree of acetylation and the electrostatic properties of chitin and chitosan, Biomacromolecules 2 (2001) 765–772.
[15] X. He, R. Yuan, Y. Chai, Y. Shi, A sensitive amperometric immunosensor for carcinoembryonic antigen detection with porous nanogold film and nano-Au/chitosan composite as immobilization matrix, J. Biochem. Biophys. Methods 70 (2007) 823–829.

[16] J.D. Lambert, R.T. Dorr, B.N. Timmermann, Nordihydroguaiaretic acid: a review of its numerous and varied biological activities, Pharm. Biol. 42 (2004) 149–158.
[17] A. Ciszewski, G. Milczarek, Electrocatalysis of NADH oxidation with an electropolymerized film of 1, 4-bis(3, 4-dihydroxyphenyl)-2, 3-dimethylbutane, Anal. Chem. 72 (2000) 3203–3209.
[18] M.H. Sorouraddin, J.L. Manzoori, E. Kargarzadeh, A.M.H. Shabani, J. Pharm, Spectrophotometric determination of some catecholamine drugs using sodium bismuthate, Biomed. Anal. 18 (1998) 877–881.
[19] M.E. El-Kommos, F.A. Mohamed, A.S.K. Khedr, Spectrophotometric determination of some catecholamine drugs using metaperiodate, J. Assoc. Off. Anal. Chem. 73 (1990) 516–520.
[20] Y. Yan, M. Zhang, K. Gong, L. Su, Z. Guo, L. Mao, Adsorption of methylene blue dye onto carbon nanotubes: a route to an electrochemically functional nanostructure and its layer-by-layer assembled nanocomposite, Chem. Mater. 17 (2005) 3457–3463.
[21] U. Yogeswaran, S.M. Chen, Electrocatalytic properties of electrodes which are functionalized with composite films of f-MWCNTs incorporated with poly(neutral red), J. Electrochem. Soc. 154 (2007) E178–E186.
[22] E. Laviron, General expression of the linear potential sweep voltammogram in the case of diffusionless electrochemical systems, J. Electroanal. Chem. 101 (1979) 19–28.
[23] T. Komura, G.Y. Niu, T. Yamaguchi, M. Asano, A. Matsuda, Coupled electron–proton transport in electropolymerized methylene blue and the influences of its protonation level on the rate of electron exchange with β-nicotinamide adenine dinucleotide, Electroanalysis 16 (2004) 1791–1800.
[24] U. Yogeswaran, S. Thiagarajan, S.M. Chen, Pinecone shape hydroxypropyl-β-cyclodextrin on a film of multi-walled carbon nanotubes coated with gold particles for the simultaneous determination of tyrosine, guanine, adenine, and thymine, Carbon 45 (2007) 2783–2796.
[25] S.M. Chen, M.I. Liu, Electrocatalytic properties of NDGA and NDGA/FAD hybrid film modified electrodes for NADH/NAD^+ redox reaction, Electrochim. Acta 51 (2006) 4744–4753.
[26] S.M. Chen, C.J. Liao, V.S. Vasantha, Preparation and electrocatalytic properties of osmium oxide/hexacyanoruthenate films modified electrodes for catecholamines and sulfur oxoanions, J. Electroanal. Chem. 589 (2006) 15–23.
[27] U. Yogeswaran, S.M. Chen, Separation and concentration effect of f-MWCNTs on electrocatalytic responses of ascorbic acid, dopamine, and uric acid at f-MWCNTs incorporated with poly(neutral red) composite films, Electrochim. Acta 52 (2007) 5985–5996.
[28] U. Yogeswaran, S.M. Chen, S.H. Li, Electroanalytical responses of arsenic oxide, methanol, and oxygen at the ruthenium oxide–hexachloroiridate with platinum hybrid film, Electroanalysis 20 (2008) 2324–2332.
[29] J. Wang, J. Dai, T. Yarlagadda, Carbon nanotube-conducting-polymer composite nanowires, Langmuir 21 (2005) 9–12.
[30] M. Tahhan, V.T. Truong, G.M. Spinks, G.G. Wallace, Carbon nanotube and polyaniline composite actuators, Smart Mater. Struct. 12 (2003) 626–632.